**Molecular Human Reproduction, Vol.21, No.8 pp. 633–644, 2015**
Advanced Access publication on May 20, 2015 doi:10.1093/molehr/gav026

molecular human reproduction

ORIGINAL RESEARCH

# Expression and characterization of three Aurora kinase C splice variants found in human oocytes

**Jessica E. Fellmeth[1], Derek Gordon[1], Christian E. Robins[2], Richard T. Scott Jr[2], Nathan R. Treff[1,2], and Karen Schindler[1,*]**

[1]Department of Genetics, Rutgers University, 145 Bevier Road, Piscataway, NJ 08854, USA [2]Reproductive Medicine Associates of New Jersey, Basking Ridge, NJ 07960, USA

*Correspondence address. Tel: +1-848-445-2563; Fax: +1-732-445-1147; E-mail: schindler@biology.rutgers.edu

*Submitted on March 31, 2015; resubmitted on May 4, 2015; accepted on May 14, 2015*

**ABSTRACT:** Chromosome segregation is an extensively choreographed process yet errors still occur frequently in female meiosis, leading to implantation failure, miscarriage or offspring with developmental disorders. Aurora kinase C (AURKC) is a component of the chromosome passenger complex and is highly expressed in gametes. Studies in mouse oocytes indicate that AURKC is required to regulate chromosome segregation during meiosis I; however, little is known about the functional significance of AURKC in human oocytes. Three splice variants of AURKC exist in testis tissue. To determine which splice variants human oocytes express, we performed quantitative real-time PCR using single oocytes and found expression of all three variants. To evaluate the functional differences between the variants, we created green fluorescent protein-tagged constructs of each variant to express in oocytes from *Aurkc*$^{-/-}$ mice. By quantifying metaphase chromosome alignment, cell cycle progression, phosphorylation of INCENP and microtubule attachments to kinetochores, we found that AURKC_v1 was the most capable of the variants at supporting metaphase I chromosome segregation. AURKC_v3 localized to chromosomes properly and supported cell cycle progression to metaphase II, but its inability to correct erroneous microtubule attachments to kinetochores meant that chromosome segregation was not as accurate compared with the other two variants. Finally, when we expressed the three variants simultaneously, error correction was more robust than when they were expressed on their own. Therefore, oocytes express three variants of AURKC that are not functionally equivalent in supporting meiosis, but fully complement meiosis when expressed simultaneously.

**Key words:** Aurora kinase C / female fertility / meiosis / oocyte maturation

## Introduction

The process of meiosis involves the formation of haploid gametes from diploid precursor cells. Mistakes in chromosome segregation during meiosis can cause aneuploidy in gametes, which is one of the leading genetic causes of infertility (Brandriff *et al.*, 1994; Hassold and Hunt, 2001; Hassold *et al.*, 2007; Pacchierotti *et al.*, 2007). These errors are sexually dimorphic; the error rate in sperm is ~5% whereas in oocytes, the rate can be upwards of 20% (Brandriff *et al.*, 1994; Hassold and Hunt, 2001; Hassold *et al.*, 2007; Pacchierotti *et al.*, 2007). This difference in error rates is not fully understood. Meiotic events in males and females are similar; however, they differ in timing. In sperm, the process occurs continuously and starts at puberty, whereas in oocytes, there is a prolonged arrest at prophase I after homologous recombination during fetal development, then resumption of meiosis at ovulation, and arrest at metaphase of meiosis II (Met II) prior to fertilization. While the result of chromosome segregation is the same between oocytes and sperm (homologs separate in meiosis I (MI) and sister chromatids separate in meiosis II (MII)), the regulation of these steps may differ. One example of a regulator that appears to function differently in male and female meiosis is Aurora kinase C (AURKC). AURKC is essential for male meiosis, but its requirement in female meiosis is not as stringent (Dieterich *et al.*, 2007).

AURKC is a serine/threonine protein kinase that regulates chromosome segregation during meiosis (Glover *et al.*, 1995; Kimmins *et al.*, 2007; Schindler *et al.*, 2012). In mice, loss of AURKC leads to subfertility, but the severity of this phenotype is not uniform between males and females. Female *Aurkc*$^{-/-}$ mice produce an average of two pups less per litter than their wildtype counterparts, while *Aurkc*$^{-/-}$ males produce seven pups less per litter and 40% are completely sterile (Kimmins *et al.*, 2007; Schindler *et al.*, 2012). In humans, AURKC is required for male meiosis because the absence of a functional protein is associated with male infertility (Dieterich *et al.*, 2007, 2009). Men with *AURKC* mutations present with macrozoospermia that is due to a

© The Author 2015. Published by Oxford University Press on behalf of the European Society of Human Reproduction and Embryology.
This is an Open Access article distributed under the terms of the Creative Commons Attribution Non-Commercial License (http://creativecommons.org/licenses/by-nc/4.0/), which permits non-commercial re-use, distribution, and reproduction in any medium, provided the original work is properly cited. For commercial re-use, please contact journals.permissions@oup.com

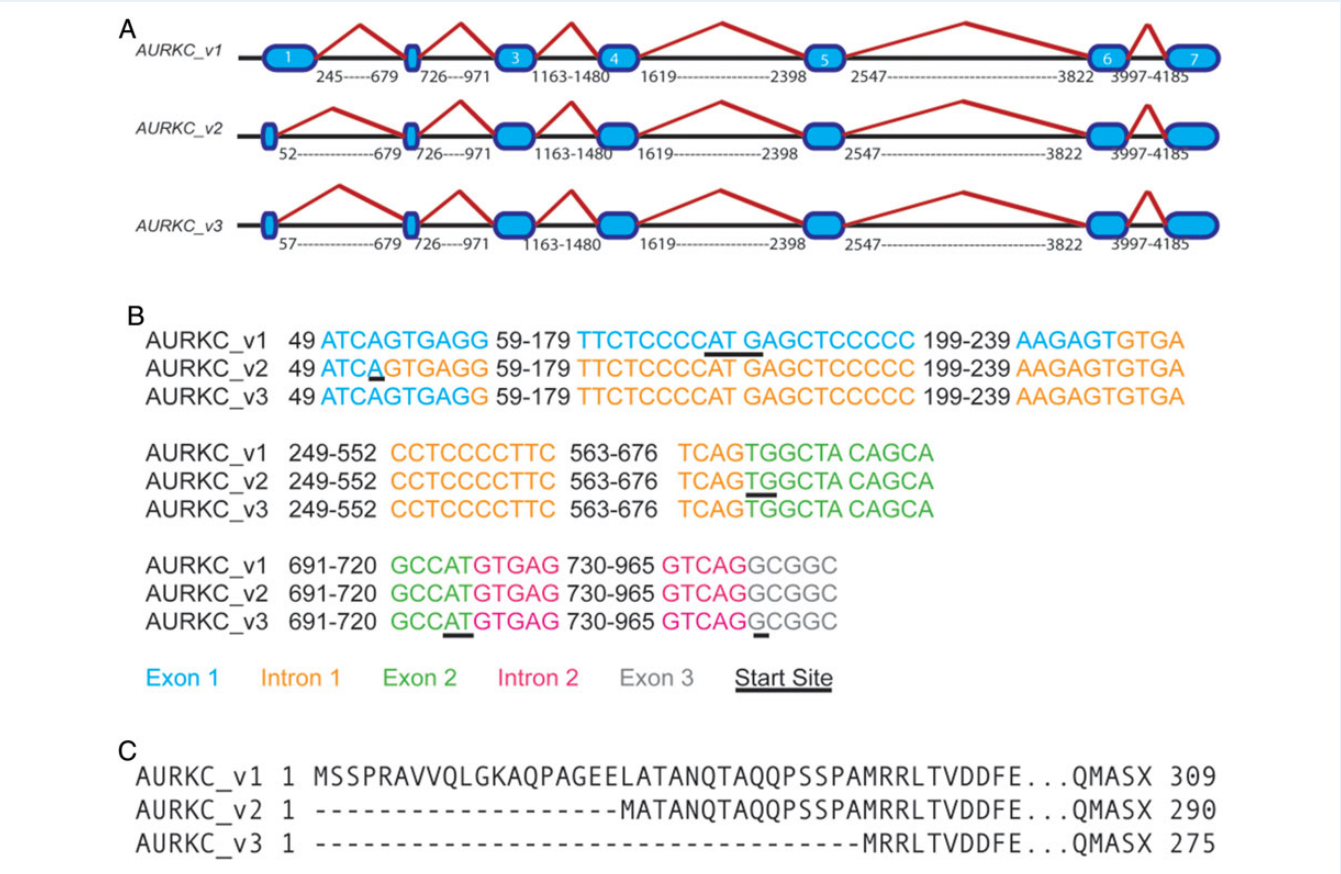


**Figure 1** *AURKC* is alternatively spliced. (**A**) Schematic illustration to show that the 5′ end of exon 1 of *AURKC* contains alternative splice sites. (**B**) Nucleotide sequence of the 5′ end of *AURKC* to highlight the alternative start sites for each splice variant. (**C**) Amino acid sequence of each variant. The kinase domain starts at residue 42.

failure to complete MI. In contrast, two women homozygous for the same sterility-associated mutations reported having no trouble conceiving (Dieterich *et al.*, 2009). Therefore, the function or effect of identified *AURKC* mutations in females is not known. A tractable model is therefore needed to gain a better understanding of the function of AURKC in female fertility.

In humans, the genomic locus of *AURKC* contains three alternative splice sites located in exon 1 (Fig. 1A and B) (Bernard *et al.*, 1998; Tseng *et al.*, 1998; Yan *et al.*, 2005). *AURKC_v1* encodes the longest transcript (Fig. 1A and B), and is more abundant in the testis relative to other tissues (Yan *et al.*, 2005). *AURKC_ v3*, identified in a screen of human placental cDNA using probes for an Aurora kinase homolog from *Xenopus laevis,* is the shortest (Fig. 1A and B) (Bernard *et al.*, 1998). *AURKC_v2* was incidentally found in a screen to isolate *AURKC_v3* (Fig. 1A) from human testis and has *in vitro* kinase activity similar to that of AURKC_v1 (Yan *et al.*, 2005). The proteins encoded by these splice variants contain identical catalytic domains at the C-terminus but their N-termini are successively shorter (Fig. 1C). While these variants exist in testis tissue, it is not known whether they are expressed in oocytes or if the truncated forms are biologically relevant.

The goals of our study were to determine which variants are expressed in human oocytes and to assess their functional relevance in female meiosis. Using quantitative RT-PCR (qRT-PCR), we observed substantially greater levels of *AURKC* expression in oocytes relative to other cell types (sperm and cumulus cells), and we amplified the three splice variants in all oocytes tested. To assess functional differences, we demonstrated that oocytes from *Aurkc*$^{-/-}$ mice can be used as a model to study human AURKC function. Finally, we showed that although the splice variants localize similarly and can support meiotic progression, they are not functionally equivalent. We show that when the three splice variants are expressed simultaneously in *Aurkc*$^{-/-}$ oocytes, that they support microtubule error correction to a greater level than when the variants are expressed alone. Therefore, we conclude that the splice variants of *AURKC* complement each other in female meiosis to optimize the process of MI chromosome segregation. Because oocytes express three variants simultaneously and sperm do not, this expression difference could begin to explain why men are more sensitive to *AURKC* mutations than women.

# Materials and Methods

## Sample collection

Oocytes and cumulus cells were processed in Cell-to-$C_t$ lysis buffer as recommended (Ambion, #4 458 236, Grand Island, USA) and stored in liquid nitrogen. Discarded sperm samples were pelleted and washed in phosphate-buffered saline (PBS) prior to RNA collection.

## Ethical approval

Human oocyte and cumulus cell samples were obtained from patients undergoing IVF treatments and collected under Internal Review Board (IRB) approval (#20 031 397) with patient consent. Discarded sperm samples were also collected under IRB approval (#20 031 397) from couples seeking IVF without a male factor diagnosis.

All animals were maintained following the Rutgers Institutional Animal Use and Care Committee (#11-032) and the National Institutes of Health guidelines.

## RNA extraction and cDNA synthesis

cDNA was synthesized from oocytes following the manufacturers protocol for the Cell-to-$C_t$ kit (Ambion, #4 458 236). Gene-specific reverse transcription was performed using Taqman assays (Applied Biosystems Hs00916672_g1, Hs04184901_m1, Hs00921878_m1, Hs00152930_m1 and Mm99999915_g1, Grand Island, USA) and a high capacity cDNA reverse transcription kit (Applied Biosystems, #4 368 814, Grand Island, USA). A pre-amplification step was also performed according to the Cell-to-$C_t$ kit. cDNA was synthesized from sperm and cumulus cell samples using the TRIzol Plus RNA purification kit (Ambion, #12183-555) and PureLink RNA mini kit (Invitrogen, #12183-18A, Grand Island, USA) followed by gene-specific RT as above.

## Quantitative PCR

Variant-specific Taqman assays were supplied by Applied Biosystems, Inc. (Foster City, USA): Hs00916672_g1 (*AURKC_v1*), Hs04184901_m1 (*AURKC_v2*) and Hs00921878_m1 (*AURKC_v3*). Assay Hs00152930_m1 was used as a control to recognize a region shared by the splice variants (between exons 4 and 5). Assay Mm99999915_g1 was used as endogenous *GAPDH* control. We confirmed Taqman probe specificity by assaying amplification of a cDNA clone for AURKC_v1. We only detected an amplification signal with the AURKC_v1 and the Taqman probe that spans exons 4 and 5 and is shared amongst the three variants. AURKC_v2 or AURKC_v3 probes anneal to 5′ UTR sequences that are not included in our cDNA clones precluding their assessment in the same manner. We also note that these probes were validated for specificity computationally by Applied Biosystems.

For each cDNA sample, duplex reactions were prepared to a final volume of 5 μl in a MicroAmp optical 384-well reaction plate (Applied Biosystems, Inc., Grand Island, USA) containing equal amounts of *GAPDH* assay, one of the *AURKC* assays and 1 μl of cDNA. Each reaction was run in triplicate. Reactions were performed on a 7900HT SDS real-time PCR instrument (Applied Biosystems, Inc., Grand Island, USA) and the default cycling conditions were used with default dissociation curve settings in the instrument control and data acquisition software (SDS version 2.3, Applied Biosystems, Inc., Grand Island, USA). RQ Manager version 1.2 data analysis software (Applied Biosystems, Inc., Grand Island, USA) was used with default settings to assign the threshold value for each reaction and results were then exported to Microsoft Excel for statistical analysis. Data were processed using the comparative $C_t$ method as previously described (Livak and Schmittgen, 2001).

## Murine oocyte preparation and microinjection

Fully-grown, GV-intact oocytes from 6- to 9-week old *Aurkc*$^{-/-}$ mice with a 129/SVpas/C57Bl/6 mixed background (Kimmins *et al.*, 2007; Schindler *et al.*, 2012) or CF-1 mice (Harlan Laboratories, #NSACF1, Indianapolis, USA) that were primed (44–48 h before collection) with pregnant mare's serum gonadotrophin (Calbiochem #367 222, Darmstadt, Germany) were collected as previously described (Anger *et al.*, 2005). Oocytes were cultured and matured as previously described (Schindler *et al.*, 2012). The collection and injection medium was bicarbonate-free minimal essential medium (MEM) containing, 25 mM Hepes, pH 7.3, 3 mg/ml polyvinylpyrollidone (MEM/PVP) and 2.5 μM milrinone (Sigma-Aldrich #M4659, St. Louis, USA) to prevent meiotic resumption (Tsafriri *et al.*, 1996). To control for mouse-to-mouse variation, denuded oocytes were kept separate for each mouse and divided equally amongst experimental groups. We injected each oocyte with 250 ng/μl of cRNA, as previously described (Anger *et al.*, 2005). After injection, oocytes were incubated overnight (for MII experiments) or for 3 h (for MI experiments) in Chatot, Ziomek and Bavister (CZB) medium containing 2.5 μM milrinone before meiotic resumption was initiated. All culture and *in vitro* meiotic maturation occurred in a humidified incubator with 5% $CO_2$ in air at 37°C. For metaphase of meiosis I (Met I) analyses, oocytes matured for 7–8 h and for Met II analyses, oocytes matured for 16 h. *In vitro* maturation was conducted in CZB medium without milrinone.

## Challenge of kinetochore-microtubule attachment correction

After 7 h of meiotic maturation, oocytes were incubated in CZB containing 100 μM monastrol (Sigma-Aldrich, #M8515) to induce monopolar spindle formation. After 2 h oocytes were washed out of the monastrol-containing media and allowed to recover in CZB containing 5 μM MG132 (Calbiochem, #47 4791) to prevent anaphase onset. After 3 h, oocytes were incubated for 7 min in pre-chilled MEM on ice to destabilize any unattached microtubules. Oocytes were fixed as described below.

## Live imaging

After microinjection, oocytes were treated with 10 μg/ml cycloheximide (Sigma-Aldrich, #C7698-1G). After 1 h, oocytes were transferred into separate drops of CZB medium with cycloheximide in a 96 well dish (Greiner Bio One, #655 892, Monroe, USA). Bright field, green fluorescent protein-tagged (GFP) (470 nm), and mCherry (585 nm) images were acquired using an EVOS FL Auto Imaging System (Life Technologies, Grand Island, USA) with a 10× objective. The microscope stage was heated to 37°C and 5% $CO_2$ was maintained using the EVOS Onstage Incubator. Images were acquired every 20 min for 10 h.

## Cloning and synthesis of cRNA

The generation of m*Aurkc-Gfp* was previously described (Shuda *et al.*, 2009). The *AURKC_v1* cDNA clone was purchased from Genecopeia (#EX-Q0034-M02-B, Rockville, USA). *AURKC_v2* was cloned via PCR from *AURKC_v1* using a forward primer (5′- GATCGCATGCATGGCTACAG-3′). *AURKC_v3* was obtained from Thermo Scientific (#160-002-F-8, Somerset, USA). All cDNA clones were PCR amplified and ligated into pIVT-EGFP (Igarashi *et al.*, 2007) using SphI and SalI. We performed *in vitro* transcription with a mMessage mMachine kit (Ambion, #AM1344M) as per the manufacturer's instructions. cRNA was purified using an RNA-Easy purification kit (Qiagen, #74 104, Venlo, Netherlands) and eluted in RNase free $H_2O$.

## Immunocytochemistry

After maturation, oocytes were fixed in PBS with 2% paraformaldehyde for 20 min at room temperature and then washed through blocking buffer (PBS + 0.3% (wt/vol) BSA + 0.01% (vol/vol) Tween-20). Prior to immunostaining, oocytes were permeabilized for 15 min in PBS containing 0.1% (vol/vol) Triton X-100 and 0.3% (wt/vol) BSA. The cells were then washed in blocking buffer (PBS + 0.3% BSA + 0.01% Tween-20). Immunostaining was performed by incubating in primary antibody; phosphorylated form of INCENP (pINCENP) [gift from M. Lampson, University of Pennsylvania (Salimian *et al.*, 2011) 1:1000], acetylated tubulin (Sigma-Aldrich, #T7451; 1:1000), CREST (Antibodies Incorporated, #15–234, Davis, USA; 1:30) or Alexa-fluor 488 conjugated alpha-tubulin (Sigma-Aldrich, #T9026; 1:100) for 1 h. After washing, secondary antibodies [anti-rabbit (Life Technologies, #A10042), anti-mouse (Life Technologies, #A10037), anti-human (Life Technologies,

#A21091)] were diluted 1:200 in blocking solution and the sample was incubated for 1 h at room temperature. After washing, the cells were mounted in VectaShield (Vector Laboratories, #H-1000, Burlingame, USA) with 4′, 6-Diamidino-2-Phenylindole, Dihydrochloride (DAPI; Life Technologies #D1306; 1:170). Fluorescence was visualized on a Zeiss 510 Meta laser-scanning confocal microscope with a 40× objective. The laser power was adjusted to just below saturation relative to the group exhibiting the highest level of signal intensity and all images were scanned at this laser power.

## Immunoblotting

Oocytes were lysed in 1% SDS, 1% β-mercaptoethanol, 20% glycerol and 50 mM Tris-HCl (ph6.8), and denatured at 95°C for 10 min. Proteins were separated by electrophoresis in 10% SDS polyacrylamide precast gel (Bio-Rad, #456-1036, Hercules, USA). Stained proteins of known molecular mass (range 10–250 kDa, Bio-Rad, #161-0376) were run simultaneously as standards. The separated polypeptides were transferred to nitrocellulose membranes (Bio-Rad, #170-4156) using a Trans-Blot Turbo Transfer System (Bio-Rad) and then blocked with 2% ECL blocking (Amersham, #RPN418, Pittsburgh, USA) solution in TBS-T (Tris-buffered saline with 0.1% Tween 20) for 1 h. The membranes were incubated with α-tubulin primary antibody (Sigma-Aldrich, #T-6074; 1:10 000) overnight or GFP primary antibody (Sigma-Aldrich, #G6539; 1:1000) for 1 h. After washing with TBS-T five times, the membranes were incubated with a secondary antibody labeled with horseradish peroxidase (GE Healthcare Biosciences, #NA931, Pittsburgh, USA) for 1 h followed with washing with TBS-T five times. The signals were detected using the ECL Select western blotting detection reagents (Amersham, #RPN2235) following the manufacturers protocol.

## Image analysis

All images were processed using ImageJ software (NIH, Bethesda, USA). Alignment measurements were performed as previously described using the same processing parameters for all images (Lane et al., 2012). In brief, we created a 4 μm box surrounding the metaphase plate that contains all aligned kinetochores. Oocytes containing kinetochores that fall outside of this box were considered 'misaligned.' pINCENP intensity measurements were performed by averaging region of interest measurements at six kinetochores per oocyte, subtracting an average of three background measurements and normalizing to average GFP expression per cell to account for injection amount. Protein stability measurements were obtained by normalizing all GFP:mCherry ratios for each time point relative to time zero.

## Statistical analysis

JMP Software was used to calculate Spearman Rank Correlation coefficients between AURKC splice variant expression in oocyte samples. One-way ANOVA or linear regression analysis as indicated in the figure legends were used to evaluate the differences between groups using Prism Graphpad software (La Jolla, USA). For experiments analyzing chromosome alignment, a permutation version of the binomial proportions test (Snedecor and Cochran, 1989) was used to analyze differences between groups. Fisher's Method (Fisher, 1925) was used to combine the results of several independent tests with the same null hypothesis. The Bonferroni correction was used to determine if the Fisher-Method *P*-values were significant after multiple testing. $P < 0.05$ was considered significant.

# Results

## *AURKC* is highly expressed in human oocytes

High *Aurkc* expression in mice is limited to germ cells (Yanai et al., 1997; Tseng et al., 1998), and its function is important for meiotic cell cycle progression (Hu et al., 2000; Chen et al., 2005; Tang et al., 2006; Yang et al., 2010; Schindler et al., 2012; Yang et al., 2013; Balboula and Schindler, 2014) and post-meiotic sperm development (Kimmins et al., 2007). However, the expression levels in single oocytes relative to other cell types and the expression of the individual splice variants is not known. To confirm the presence of *AURKC* and to interpret relative quantities of expression in human oocytes, we performed qRT-PCR on cDNA from single oocyte samples, each from a different donor patient with paired cumulus cell samples (Table I). Human sperm samples were used as controls. After calculating the percent fold change relative to endogenous *GAPDH* message, the data demonstrate the presence of *AURKC* transcript in every oocyte sample tested, in agreement with previous findings (Assou et al., 2006; Grondahl et al., 2010; Avo Santos et al., 2011) (Fig. 2). Although it is an interesting question to ask, our current sample size was too limited to make correlations between age and expression of *AURKC*.

**Table I GV-arrested oocytes were obtained along with follicular fluid from the same donors**

| Patient age (years) | Cell type | Stage | Symbol |
|---|---|---|---|
| 34.1 | Oocyte Cumulus | GV | ■ |
| 34.4 | Oocyte Cumulus | GV | ★ |
| 34.7 | Oocyte Cumulus | GV | ▼ |
| 36.2 | Oocyte Cumulus | GV | ▲ |
| 37.4 | Oocyte Cumulus | GV | ✱ |
| 38.3 | Oocyte Cumulus | GV | ⬢ |
| 38.8 | Oocyte Cumulus | GV | ● |
| 40.5 | Oocyte Cumulus | GV | ◆ |

Each donor is annotated with a symbol so sample information can be found on each relevant graph in Figs 2 and 3.

We detected *AURKC* in cDNA samples from sperm and cumulus cells (Fig. 2). The sperm cDNAs tested expressed *AURKC*, with an average expression level of 2-fold greater than expression of *GAPDH*. This expression level is substantially lower than the expression level in oocytes (Fig. 2). Similar to oocytes, the levels of expression of *AURKC* in sperm from donor to donor varied ranging from 6-fold greater to 10-fold lower relative to *GAPDH* expression (Fig. 2). Because the expression level of *AURKC* was higher in oocytes than it was in sperm, these data suggest differential requirements for the protein in male and female meiosis.

We also detected *AURKC* in cumulus cells at levels similar to those previously described (Assou et al., 2006). The expression levels were markedly lower (~1000 and ~20-fold) compared with levels in oocytes and sperm, respectively (Fig. 2). There was no correlation between the abundance of *AURKC* transcript in oocytes to that in cumulus cells from the same patient (Fig. 2, Spearman Rank Correlation Test, $P = 0.5$). *AURKC* is expressed at low levels in placental, lung and some tumor tissue samples (Yan et al., 2005; Baldini et al., 2011), but

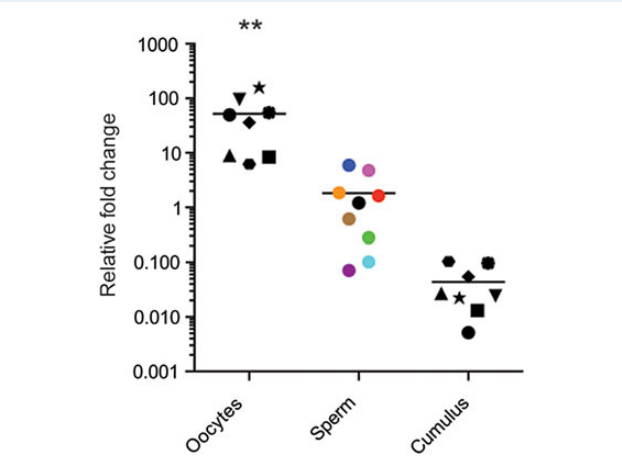


**Figure 2** *AURKC* is more highly expressed in oocytes than in sperm or cumulus cells. qRT-PCR was performed on human samples to measure total *AURKC* expression using $2^{-\Delta Ct}$. The symbols in oocyte and cumulus represent the individual donors in Table I. The different colors used in the sperm samples represent each donor for ease of identification and comparison with Fig. 3A. The average bar represents the mean level of expression. One-way ANOVA was used to analyze data. $^{**}P = 0.005$.

not at significant levels in any other mitotic tissues in humans. Its expression in cumulus cells could indicate a more involved role for AURKC in the cumulus-oocyte complex in supporting oocyte growth or meiotic progression.

## Human oocytes express three variants of *AURKC*

Three *AURKC* splice variants are expressed in human testis tissue (Bernard *et al.*, 1998; Tseng *et al.*, 1998; Yan *et al.*, 2005). To determine which splice variants are expressed in oocytes, we verified that the variant-specific Taqman assays detect and amplify each transcript. To this end, we generated human sperm cDNA libraries expected to contain the three transcripts. The data indicate that *AURKC_v1* was present in all sperm samples tested, whereas *AURKC_v2* and *AURKC_v3* were detected in three and four of the nine samples, respectively (Fig. 3A). No sample expressed the three variants simultaneously.

Next, we used the variant-specific Taqman probes to determine which splice variants were present in the oocyte samples. Each splice variant was detected in every oocyte lysate (Fig. 3B, Table I). The average expression level for each variant was 7.7, 1.8 and 4.5 fold greater than *GAPDH,* respectively. Using the comparative $C_t$ method, we determined that *AURKC_v1* was the most abundant, making up ~47.8% of the total *AURKC* composition in oocytes and *AURKC_v2* was expressed at the lowest level, making up ~14.5% (Fig. 3B and C). We note that there was variation amongst expression levels between samples (Fig. 3B). Variation of *AURKC_v1* ranged from 5-fold less to 15-fold greater expression than *GAPDH*. Variants 2 and 3 ranged from 9-fold less to 12-fold more and equal to 22 times more than *GAPDH*, respectively. Similar to the results with the amount of total *AURKC* (Fig. 2), there was variation in the amounts of each transcript in oocytes from different donors. Even within the same oocyte, there was variability in expression of the three variants. For example, the oocyte from the 34.7-year-old donor expressed above average levels of *AURKC_v1* and *AURKC_v3* but below average levels of *AURKC_v2* (Fig. 3B, Table I). The significance of the variability from patient to patient is unknown, and outside the scope of this study. All oocytes tested expressed each splice variant while sperm samples most commonly expressed variant 1. This change in expression further supports the model of differential function for AURKC in oocytes and sperm.

*AURKC* is expressed at low levels in cumulus cells (Assou *et al.*, 2006); therefore, we wanted to investigate the splice variant composition of the mitotic cell counterparts of the oocytes tested. Using the same variant-specific Taqman assays, we detected the expression of *AURKC_v1* in cumulus cell samples (Fig. 3D). Similar to total *AURKC* expression, there was no correlation between variant expression levels in cumulus cells and oocytes from the same patient (Spearman Rank Correlation Test, $P = 0.13$). Therefore, mitotic cycling cumulus cells expressed *AURKC*, however, they only expressed splice variant 1.

## Splice variants are differentially stable during meiosis

The existence of three splice variants of *AURKC* indicates the need for different functions in meiosis but these specific roles are unclear. We hypothesized that the splice variants could have different stability properties. To test this hypothesis, we monitored oocytes from wildtype mice, expressing GFP-tagged variants and treated with cycloheximide, via live-imaging and quantified fluorescence over the course of 10 h. We found that AURKC_v2 was significantly more stable over the time course than either AURKC_v1 or AURKC_v3 (Fig. 4). Because the only difference in these variants is the length of the N-terminus, these results indicate the presence of a destruction motif between residues 1–19 that is lacking in AURKC_v2, and a region that imparts stability between residues 20–34 that AURKC_v3 is lacking (Fig. 1C). This hypothesis is supported by the data showing that the initial destruction ($t = 0–2$ h) of AURKC_v3 is faster (slope $= -0.1757$) than the initial destruction of AURKC_v1 (slope $= -0.1149$) (Fig. 4). A search for similar motifs has not yielded any significant findings, indicating that these are presently unidentified domains.

## *Aurkc*$^{-/-}$ mouse oocytes as a model for studying human *AURKC* in meiosis

To determine the biological significance of the variants, we first established a model to assay AURKC function. Oocytes from *Aurkc*$^{-/-}$ mice have distinct meiotic phenotypes that are quantifiable and make it a convenient model for studying AURKC function in meiosis. These phenotypes include arrest at metaphase of MI with chromosome misalignment (Schindler *et al.*, 2012), reduced levels of pINCENP (the AURKB and AURKC substrate) and increased frequency of errors in kinetochore-microtubule attachments (K-MT attachments) (our unpublished observations). Because human (hAURKC) and mouse (mAURKC) AURKC share 87% homology in the catalytic domain, we hypothesized that hAURKC could complement the defects of oocytes from *Aurkc*$^{-/-}$ mice.

To test this hypothesis, we compared the phenotypic rescue of oocytes lacking AURKC that were microinjected with either mouse

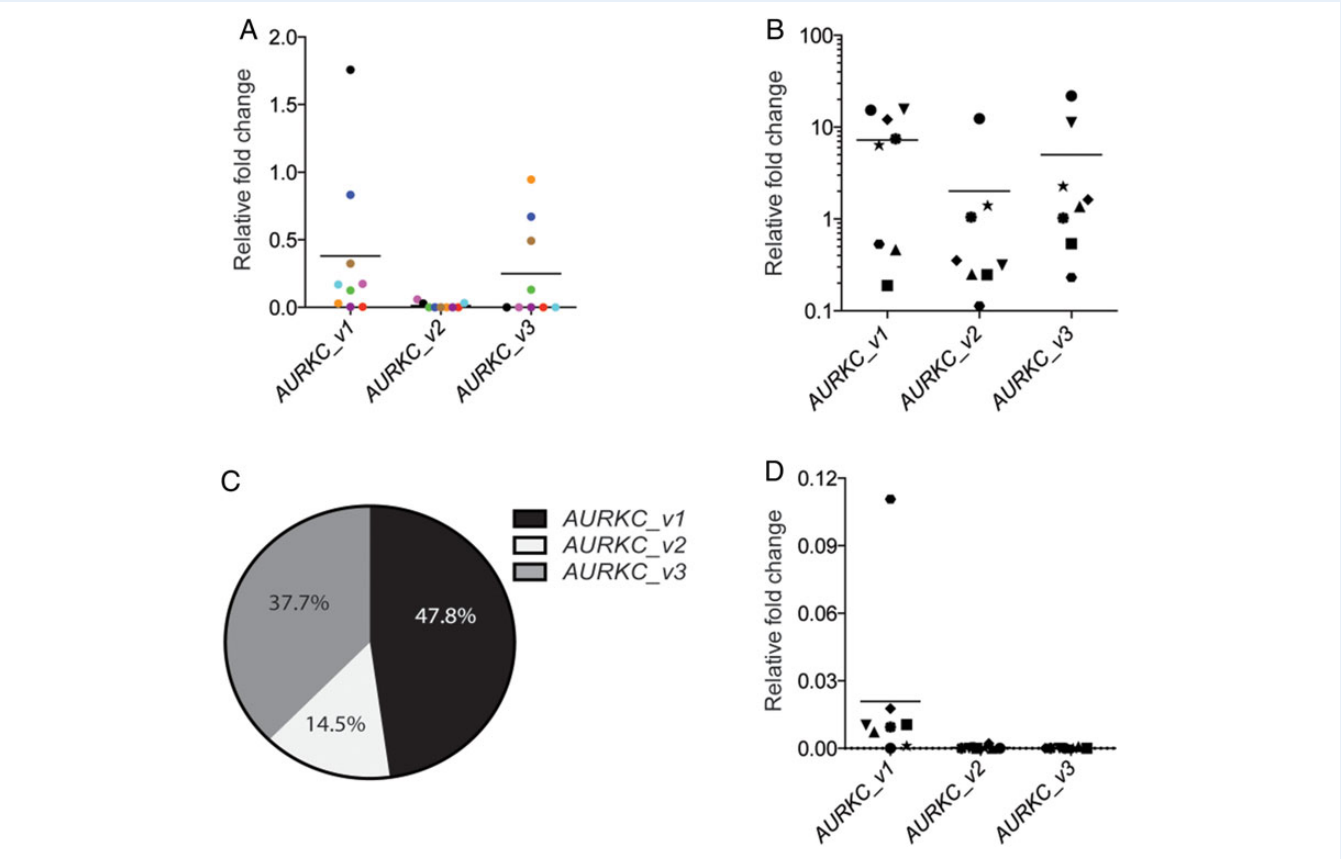


**Figure 3** Oocytes express three splice variants while sperm and cumulus cells express 1. (**A**, **B** and **D**) qRT-PCR was performed on human samples to measure variant-specific *AURKC* expression using $2^{-\Delta Ct}$. The symbols in oocyte (B) and cumulus (D) represent the individual donors in Table I. The different colors used in the sperm samples (A) represent each donor for ease of identification. The average bar represents the mean level of expression. (**C**) Average relative expression of splice variants in oocytes using $2^{-\Delta\Delta Ct}$.

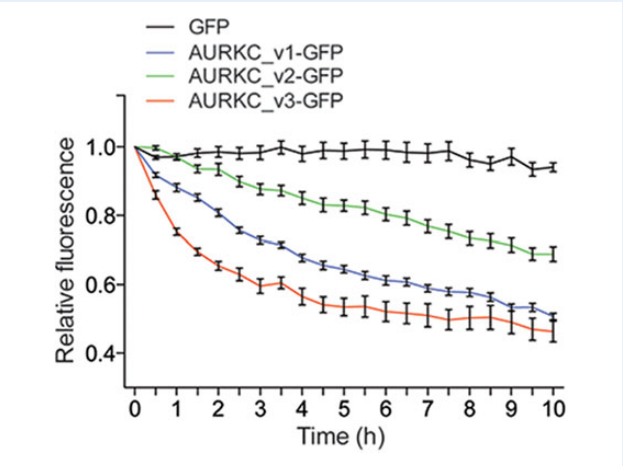


**Figure 4** AURKC splice variants differ in stability during meiotic maturation. Fully grown oocytes arrested at prophase of MI from CF-1 mice were co-injected with the indicated *Gfp*-tagged and *mCherry* cRNAs. One hour after cycloheximide addition, fluorescent images were obtained at 30 min intervals. Data points represent a mean (±SEM) from at least 20 oocytes from two independent experiments. Data were analyzed using linear regression; $P < 0.0001$.

AURKC or human AURKC_v1 *Gfp*-tagged cRNA. Endogenous and ectopically expressed mAURKC localizes along the interchromatid axis (ICA) and at the inner kinetochore during Met I, moves to the spindle midzone during telophase I (Telo I), and then back to the kinetochore at Met II (Shuda *et al.*, 2009; Sharif *et al.*, 2010; Yang *et al.*, 2010; Avo Santos *et al.*, 2011) (Fig. 5A–C). Ectopically expressed hAURKC had an identical localization as mAURKC when expressed in *Aurkc*$^{-/-}$ oocytes; along the ICA and at kinetochores at Met I, at the spindle midbody at Telo I and back to kinetochores at Met II (Fig. 5A–C). To confirm that hAURKC is active at this localization, we quantified the relative fluorescence of an antibody that recognizes the pINCENP at kinetochores of images obtained via confocal microscopy. Compared with the *Gfp*-injected control, oocytes expressing mAURKC or hAURKC had significantly increased pINCENP levels (~2-fold). Importantly, we found similar levels of INCENP phosphorylation in oocytes injected with *mAurkc* or *hAURKC* indicating that hAURKC phosphorylates mouse INCENP to a similar extent as mAURKC (Fig. 5A–D). Approximately 60% of control-injected *Aurkc*$^{-/-}$ oocytes had chromosomes that were misaligned at the Met I plate [Fig. 5E; (Schindler *et al.*, 2012)]. We found that this phenotype can be rescued by overexpression of mouse or human AURKC (Fig. 5E), indicating that hAURKC functionally complements the loss of mAURKC in *Aurkc*$^{-/-}$ oocytes. Therefore, we used these assays to assess human AURKC function in female meiosis.

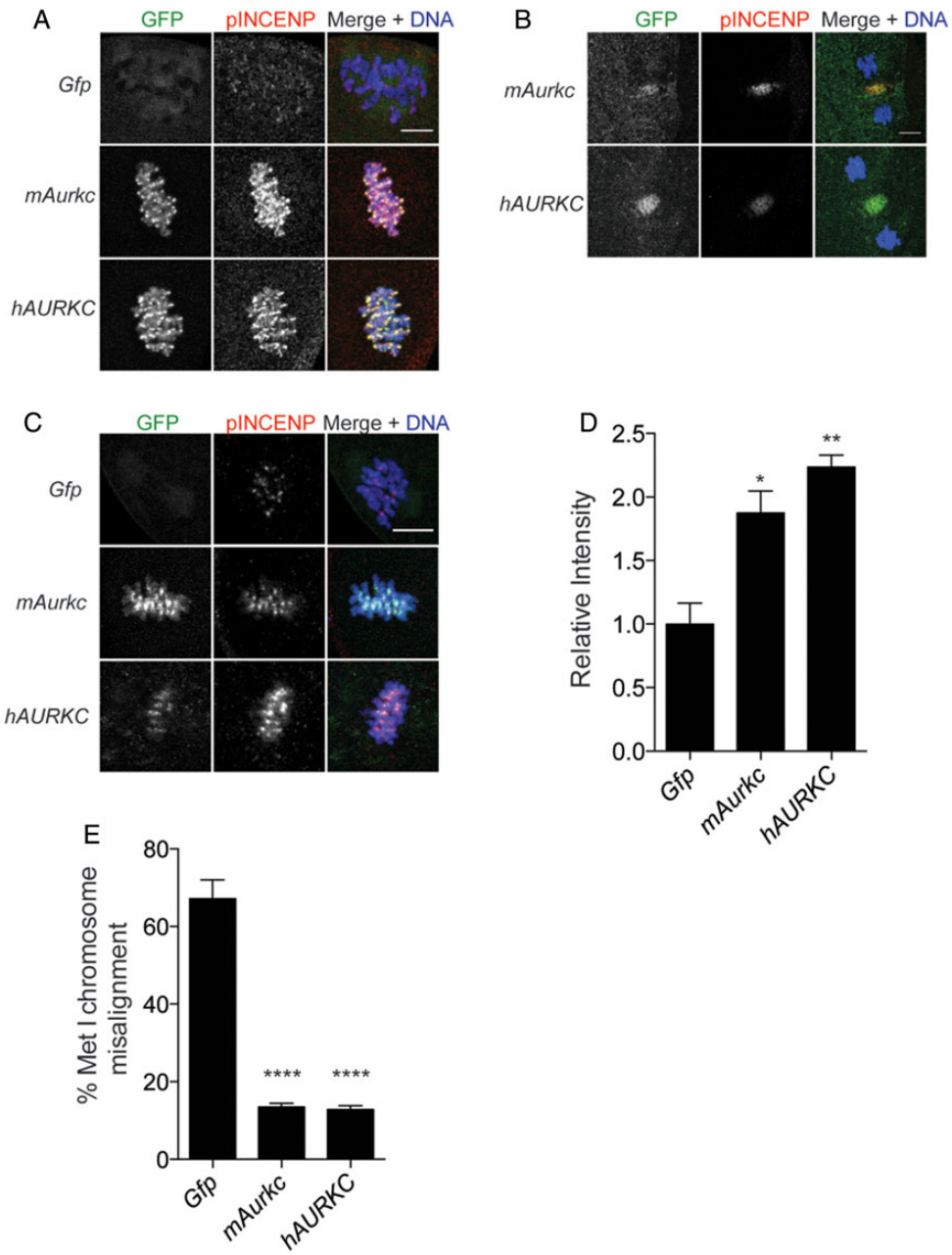


**Figure 5** Human AURKC functionally complements mouse AURKC. Fully grown oocytes arrested at prophase of MI from *Aurkc*$^{-/-}$ mice were injected with the indicated *Gfp*-tagged cRNA and matured to Met I (**A**), Telo I (**B**) or Met II (**C**) prior to fixation and immunocytochemistry to detect pINCENP (red in merge). (A–C) Representative confocal z-projections of oocytes. DNA was detected by DAPI staining (blue). Detection of GFP is green in the merge. Scale bars represent 10 μm. (**D**) Relative intensity of pINCENP at centromeres from experiments depicted in (A) after normalization with the intensity in the *Gfp* control group at Met I. One-way ANOVA was used to analyze the data and error bars represent the mean (± SEM); $^{**}P = 0.0043$, $^{****}P = 0.0005$. (**E**) Misaligned chromosomes at Met I were identified as described in Lane *et al.* Each experiment was performed three times using two mice each time. A permutation version of the binomial proportions test was used to analyze differences between groups as described in Materials and Methods section. $^{*}P = 0.0134$, $^{**}P = 0.0055$.

## *hAURKC* splice variants localize in mouse oocytes and support meiotic progression

To determine if the N-termini dictate different localization or function, we injected cRNA of *Gfp*-tagged constructs for each variant into *Aurkc*$^{-/-}$ oocytes; *Gfp* was injected as a control. At Met I, each variant localized to kinetochores and along the ICA (Fig. 6A). At Met II, localization occurred strictly at kinetochores and did not differ between the variants (Fig. 6B). We also noted dynamic localization of the AURKC variants to the spindle midbody during Telo I (Fig. 6C). Therefore, the length of the N-terminus did not affect the localization of AURKC.

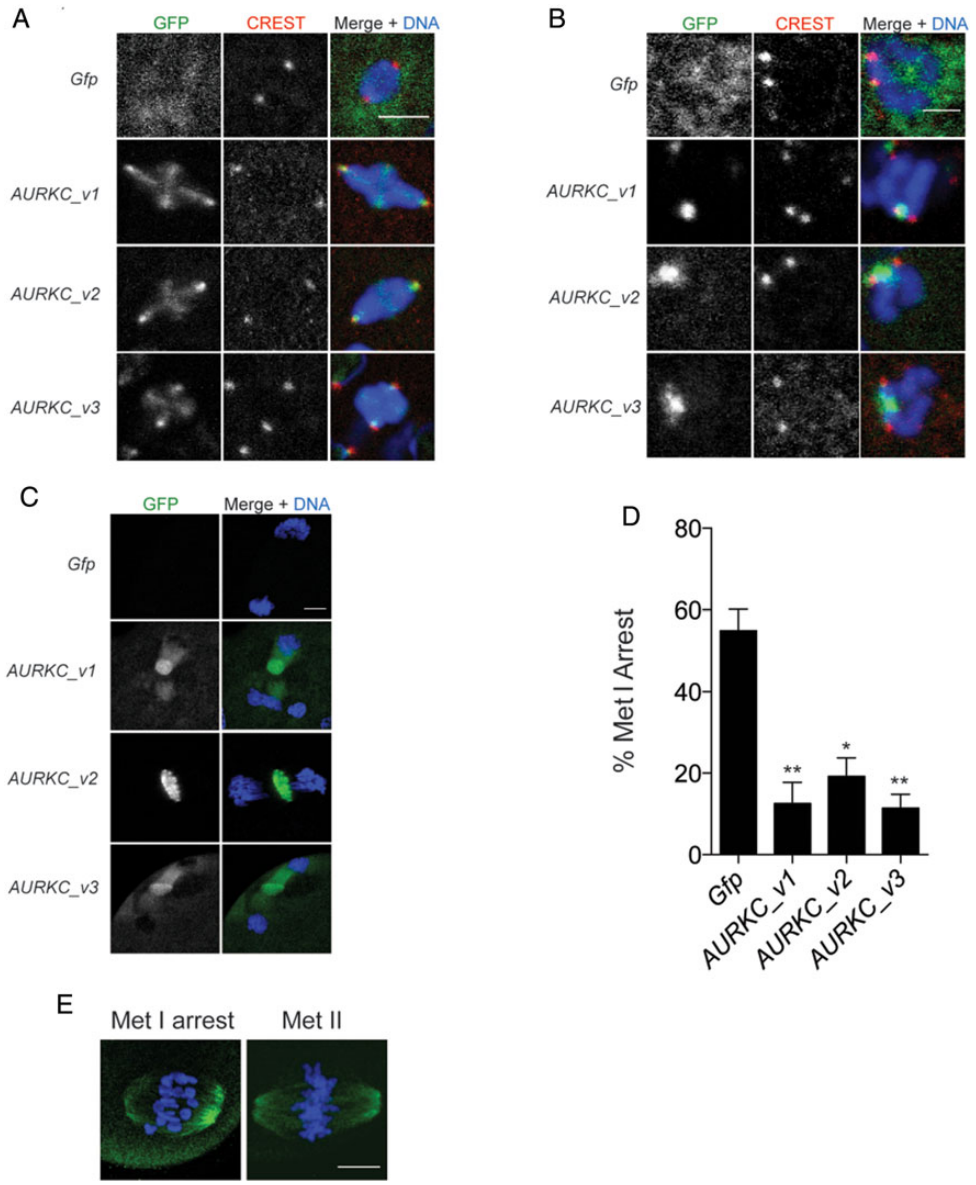


**Figure 6** AURKC splice variants have identical localization and support meiotic progression. Fully grown oocytes arrested at prophase of MI from *Aurkc*$^{-/-}$ mice were injected with the indicated *Gfp*-tagged cRNA and matured to Met I (**A**), Met II (**B**) or Telo I (**C**) prior to fixation and immunocytochemistry to detect the outer region of the kinetochore (CREST) (red in merge). (A–C) Representative confocal z-projections of oocytes. DNA was detected by DAPI staining (blue). Detection of GFP is green in the merge. (**D** and **E**) Oocytes were matured for 16 h prior to fixation and immunocytochemistry to detect the spindle (green). After acquiring images on the confocal, Met I arrest was scored by the presence of bivalents (blue). Scale bars represent 10 μm. Each experiment was performed three times using two mice each time. One-way ANOVA was used to analyze the data and error bars represent the mean (±SEM); $^{*}P = 0.0190$, $^{**}P = 0.0012$ and 0.0047, respectively.

Oocytes lacking *Aurkc* do not support meiotic maturation to the same extent as wildtype oocytes (Schindler *et al.*, 2012). As a measure of meiotic progression, we quantified *Aurkc*$^{-/-}$ mouse oocytes injected with cRNA for each variant arrested at Met I after 16 h of maturation. We found that the three splice variants significantly improved the Met I arrest phenotype witnessed in the control-injected *Aurkc*$^{-/-}$ oocytes (54%) and to the same degree (Fig. 6D). Therefore, the three splice variants all localize and support meiotic progression similarly.

## AURKC splice variants differ in supporting chromosome segregation

To further investigate the function of the variants during meiosis, we quantified the ability of each variant to phosphorylate INCENP. We injected *Aurkc*$^{-/-}$ oocytes with *Gfp* as a control. Regardless of the variant injected, the fluorescence intensity of pINCENP was significantly higher than in control-injected oocytes (Fig. 7A and B). Furthermore, *AURKC_v1*-injected oocytes had higher pINCENP immunoreactivity

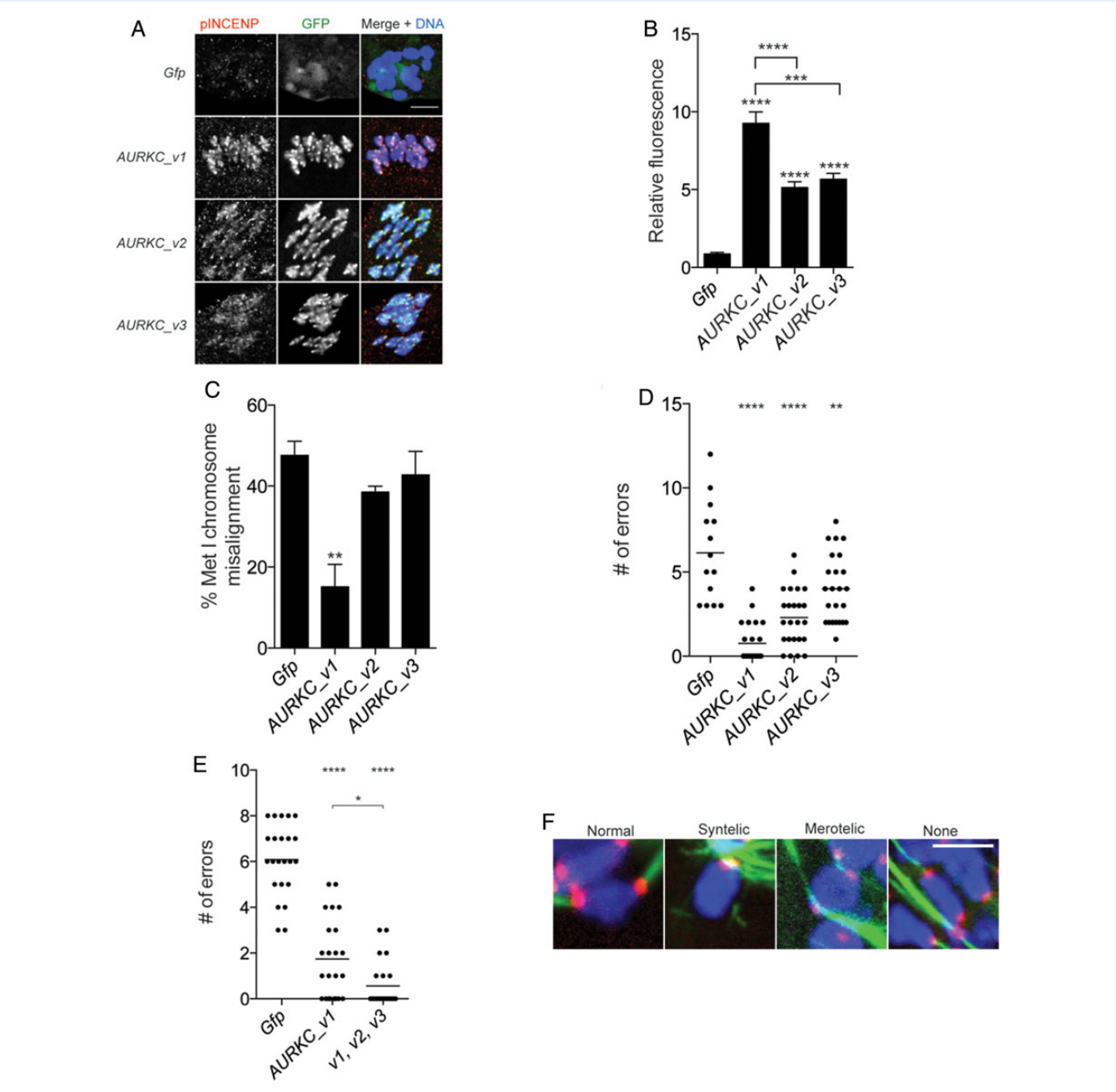


**Figure 7** AURKC splice variants differ in catalytic activity. Fully grown oocytes arrested at prophase of MI from *Aurkc*$^{-/-}$ mice were injected with the indicated *Gfp*-tagged cRNA and matured to Met I. (**A**–**C**) Oocytes were fixed and immunocytochemistry was used to detect pINCENP (red in merge). (A) Representative confocal z-projections. DNA was detected by DAPI staining (blue). Detection of GFP is green in the merge. Scale bars represent 10 μm. (B) Quantification of experiments in (A) after normalization with the intensity in the *Gfp* control group. (C) Quantification of chromosome alignment from experiments in (A) as described in Lane *et al* and our Materials and Methods section. Each experiment was performed three times using two mice each time. A permutation version of the binomial proportions test was used to analyze differences between groups as described in Materials and Methods section. *$P = 0.0057$. Variants 2 and 3 were not significantly different from the *Gfp* control ($P = 0.7233$, and 0.8697, respectively). (**D**–**F**) After maturation to Met I, oocytes were treated with monastrol for 2 h followed by a 3 h recovery. Prior to fixation, oocytes were incubated in ice-cold medium. After fixation, stable K-MT attachments were detected by immunocytochemistry to visualize spindle fibers (α-tubulin; green) and kinetochores (CREST; red). (D and E) Each data point represents the number of improper K-MT attachments quantified in a single oocyte image. (F) Representative confocal z-projections of types of K-MT attachments. Full images are shown in Supplementary data, Fig. S2. Normal attachments are classified as a chromosome containing two pairs of sister kinetochores attached to opposite poles. Syntelic attachments occur when both pairs of sister kinetochores are attached to the same pole. Merotelic attachments occur when one pair of sister kinetochores is attached to both poles. The scale bar is 5 μm. The experiments were performed twice with a total of four mice (D) or three times with a total of five mice (E). One-way ANOVA was used to analyze the data and error bars represent the mean (± SEM); *$P = 0.0143$ and 0.0329, respectively, **$P = 0.007$, ***$P = 0.0002$, ****$P < 0.0001$.

than in those injected with *AURKC_v2* or *AURKC_v3* at both Met I (Fig. 7A and B) and Met II (data not shown). These data demonstrate that AURKC_v2 and AURKC_v3 have reduced catalytic activity compared with AURKC_v1. Therefore, the length of the N-terminus appears to influence the ability of AURKC to phosphorylate substrates.

AURKC also regulates alignment of chromosomes at the metaphase plate (Sharif *et al.*, 2010; Yang *et al.*, 2010; Balboula and Schindler, 2014). Therefore, we next asked if the GFP-tagged variants rescued Met I chromosome alignment in *Aurkc*$^{-/-}$ mouse oocytes. In the *Gfp*-injected *Aurkc*$^{-/-}$ oocytes, Met I chromosome misalignment was observed 48% of the time (Fig. 7C). Despite their ability to progress through meiosis, the variant-injected oocytes did not regulate chromosome alignment to the same extent as one another (Fig. 7C). Chromosomes in *AURKC_v1*-injected oocytes were significantly more aligned than in those in oocytes injected with *AURKC_v2* or *AURKC_v3* (Fig. 7C). We also found that neither *AURKC_v2* nor *AURKC_v3*-injected oocytes could significantly improve alignment relative to the *Gfp*-injected control oocytes (Fig. 7C). These data suggest that the reduction of catalytic activity alters chromosome alignment without affecting cell cycle progression.

In order to ensure that these differences in activity were not due to differences in expression of the injected cRNAs, we performed Western blot analysis on oocytes injected with each cRNA and probed for the GFP tag (Supplementary data, Fig. S1A). We found no differences in expression between variants (Supplementary data, Fig. S1B).

One of the causes of misaligned chromosomes at the metaphase plate could be incorrect attachments between the kinetochore and the spindle microtubules (K-MT) (Brunet *et al.*, 1999; Lampson *et al.*, 2004; Balboula and Schindler, 2014). A function of AURKC in meiosis is to destabilize the incorrect attachments so that new and correct attachments can form (Balboula and Schindler, 2014). Therefore, we assayed the ability of each variant to correct erroneous K-MT attachments in *Aurkc*$^{-/-}$ mouse oocytes. These Met I oocytes were treated with monastrol, an Eg5 kinesin inhibitor, to form 100% incorrect K-MT attachments and correction was assessed after wash out of monastrol. Control-injected oocytes fixed most of the induced syntelic attachments (Fig. 7D–F, Supplementary data, Fig. S2); however, we never observed an *Aurkc*$^{-/-}$ control oocyte that fixed all of the attachments, consistent with the model that AURKC is required for this activity (Balboula and Schindler, 2014). *AURKC_v3*-injected oocytes also failed to correct all errors and frequently contained oocytes with at least three improper K-MT attachments (Fig. 7D, Supplementary data, Fig. S2). Some oocytes expressing AURKC_v1 and AURKC_v2 corrected all the syntelic attachments (44 and 16%, respectively) while the AURKC_v1 group had no oocytes with greater than three errors (Fig. 7D, Supplementary data, Fig. S2). Consistent with different levels of catalytic activity, these data demonstrate that the three splice variants differ in their ability to correct K-MT attachments.

Because human oocytes express three splice variants simultaneously, we asked if the error correction could be improved further if all three variants were expressed in *Aurkc*$^{-/-}$ oocytes at approximately the same ratio (48%:15%:37%) that we find in human oocytes (Fig. 3C). Compared with *Gfp* and variant one-injected controls, we found significant improvement in the number of oocytes that could fix all of the improper K-MT attachments when oocytes express the three variants simultaneously (Fig. 7E, Supplementary data, Fig. S2). These data imply that the three variants complement each other in function during meiosis and all three are needed for optimal fidelity of chromosome segregation.

# Discussion

The presence of AURKC in oocytes was previously determined by gene expression profiling (Assou *et al.*, 2006) and qPCR (Avo Santos *et al.*, 2011), and data from microarray analyses identified *AURKC* transcript in lysates from 15 individual oocytes samples (Grondahl *et al.*, 2010). In this study, we show that *AURKC* expression in single oocyte samples is significantly greater than that in sperm, indicating a differential requirement for the transcript in spermatogenesis and oogenesis.

Three AURKC splice variants are expressed in testis and sperm (Bernard *et al.*, 1998; Tseng *et al.*, 1998; Yan *et al.*, 2005). Here we demonstrate that the three variants are also always found in oocytes (Fig. 3B) while not all sperm samples express the three splice variants simultaneously (Fig. 3A). The differential expression of *AURKC* splice variants in gametes gives credence to the hypothesis that these variants perform different functions in female versus male meiosis. The observation that mutations in *AURKC* are correlated with infertility in men but not women is further proof that AURKC functions differently in oocytes and sperm (Dieterich *et al.*, 2007).

*AURKC_v1* is expressed in all oocytes, sperm and cumulus cells tested (Fig. 3A, B and D), but oocytes express significantly more *AURKC* than the other cell types (Fig. 2). Even the oocyte with the least amount of transcript contained ~8-fold more *AURKC* than the sperm sample with the highest levels of expression (Fig. 2). The prolonged time frame for completion of meiosis in females compared with males would necessitate a greater abundance of transcripts to account for degradation over time. At the onset of puberty, spermatogenesis occurs daily and takes ~2 months to complete and meiosis only takes ~1 day. Oogenesis, on the other hand, begins during fetal development and is not completed until after fertilization taking 12–50 years from start to finish. This prolonged delay is accompanied by transcriptional silencing (Matzuk and Lamb, 2002; Edson *et al.*, 2009). Therefore, all RNA messages required for meiosis and early embryogenesis must persist in oocytes for longer than any such transcript in sperm. The stability of these transcripts is imperative for formation of a healthy embryo, and having an abundance of *AURKC* may be advantageous for this process.

Multiple versions of a single gene may impart a benefit on oocytes by protecting against non-specific degradation. For example, as cells age, there is an increase in reactive oxygen species released by the mitochondria which in turn will attack methionines, cysteines and other aromatic residues on proteins (Imlay, 2003). Therefore, having a reserve stock of protein could allow the cell to continue normal function even in the presence of age-related oxidative stress. We hypothesize that this might be one explanation for the presence of multiple AURKC variants.

AURKC is more stable than AURKB in mouse oocytes, which provides sustained Aurora kinase activity to help support meiosis and embryonic mitoses (Schindler *et al.*, 2012). While all the variants can support meiotic progression (Fig. 6D), they are not able to do so with equal efficiency (Fig. 7). Yet, when they are combined, the overall error correction activity is greater than when any variant is expressed alone (Fig. 7E), indicating a need for the three variants to be expressed concurrently for optimal function. The variants are not found simultaneously in sperm indicating this cumulative effect is not necessary for spermatogenesis. We have not yet examined the function of these variants in older or stressed

oocytes, which could further illuminate variable function between the splice variants.

Based on known AURKB mitotic substrates that are present in mouse oocytes, there are a number of candidate targets of AURKC. The phenotypic differences we observed between the variants could be due to different affinities for these substrates. For example, Mitotic centromere-associated kinesin (MCAK) is an AURKB substrate in mitosis. AURKB-activated MCAK is responsible for the depolymerization of plus-ends microtubules to facilitate error correction, primarily merotelic attachments (Kline-Smith *et al.*, 2004; Cimini *et al.*, 2006; Wordeman *et al.*, 2007). MCAK localizes to centromeres in oocytes and therefore it is a likely AURKC substrate (Ems-McClung *et al.*, 2007; Zhang *et al.*, 2007; Vogt *et al.*, 2010). Loss of MCAK in meiotic cells results in delayed chromosome congression and potentially increased errors in K-MT attachments (Illingworth *et al.*, 2010; Vogt *et al.*, 2010). If each variant of AURKC had different affinities for MCAK, error correction at kinetochores would vary, which is consistent with our observations. Another candidate substrate at kinetochores in oocytes is HEC1 (DeLuca *et al.*, 2011; Sun *et al.*, 2011), which is involved in bipolar spindle formation and chromosome congression (Sun *et al.*, 2011; Gui and Homer, 2012). The variants do not show differences in spindle formation but chromosome alignment did vary, making differential affinity for HEC1 a possibility. Due to the relationship of AURKB and the spindle assembly checkpoint protein, MAD2, in mitosis, it is likely a downstream effector of AURKC in oocyte meiosis. Just prior to anaphase I, all kinetochores lose MAD2 even when incorrect attachments are still present (Gui and Homer, 2012). If the variants differ in their ability to correct attachments, the checkpoint would still be satisfied and polar body extrusion would occur, consistent with our observations. Therefore, differences in substrate affinity, either to these candidates or unknown meiosis-specific substrates, is a feasible mechanism to explain our results.

Mutations in *AURKC* are linked to male infertility and cancer (Kimura *et al.*, 1999; Takahashi *et al.*, 2000; Sasai *et al.*, 2004; Dieterich *et al.*, 2007). *AURKC* is a germ-cell specific transcript that has not been well characterized in oocytes. We developed an effective mouse model for studying human AURKC in oocytes. We also found that human oocytes express three splice variants but at different levels and that they function differently, yet additively, in meiosis. This could be due to differing stability and activity. Understanding the expression pattern and function of AURKC variants will shed light on the differences between male and female meiosis and genetic causes of infertility (Edson *et al.*, 2009). If causative, this information could ultimately help develop diagnostic tools for better oocyte and embryo selection in the clinic.

# Supplementary data

Supplementary data are available at http://molehr.oxfordjournals.org/.

# Acknowledgements

The authors would like to thank the members of the Schindler, McKim and Treff labs for helpful discussions. We thank Dr Michael Lampson (University of Pennsylvania) for the phospho-specific INCENP antibody and Dr David Axelrod (Rutgers University) for advice on correlation analyses.

# Authors' roles

J.E.F., K.S. and N.R.T. conceived and designed the experiments. J.E.F. and C.E.R. performed the experiments. J.E.F., D.G., N.R.T. and K.S. analyzed the data. K.S., R.T.S. and N.R.T. contributed reagents, materials or analysis tools. J.E.F. and K.S. wrote the paper.

# Funding

This work was supported by a Research Grant from the American Society for Reproductive Medicine and support from the Charles and Johanna Busch Memorial Fund at Rutgers, the State University to K.S. Funding to pay the Open Access publication charges for this article was provided by Rutgers University Institutional Start up funding.

# Conflicts of interest

None declared.

# References

Anger M, Stein P, Schultz RM. CDC6 requirement for spindle formation during maturation of mouse oocytes. *Biol Reprod* 2005;**72**:188–194.

Assou S, Anahory T, Pantesco V, Le Carrour T, Pellestor F, Klein B, Reyftmann L, Dechaud H, De Vos J, Hamamah S. The human cumulus-oocyte complex gene-expression profile. *Hum Reprod* 2006;**21**:1705–1719.

Avo Santos M, van de Werken C, de Vries M, Jahr H, Vromans MJ, Laven JS, Fauser BC, Kops GJ, Lens SM, Baart EB. A role for Aurora C in the chromosomal passenger complex during human preimplantation embryo development. *Hum Reprod* 2011;**26**:1868–1881.

Balboula AZ, Schindler K. Selective disruption of aurora C kinase reveals distinct functions from aurora B kinase during meiosis in mouse oocytes. *PLoS Genet* 2014;**10**:e1004194.

Baldini E, Arlot-Bonnemains Y, Sorrenti S, Mian C, Pelizzo MR, De Antoni E, Palermo S, Morrone S, Barollo S, Nesca A *et al.* Aurora kinases are expressed in medullary thyroid carcinoma (MTC) and their inhibition suppresses in vitro growth and tumorigenicity of the MTC derived cell line TT. *BMC Cancer* 2011;**11**:411.

Bernard M, Sanseau P, Henry C, Couturier A, Prigent C. Cloning of STK13, a third human protein kinase related to Drosophila aurora and budding yeast Ipl1 that maps on chromosome 19q13.3-ter. *Genomics* 1998;**53**:406–409.

Brandriff BF, Meistrich ML, Gordon LA, Carrano AV, Liang JC. Chromosomal damage in sperm of patients surviving Hodgkin's disease following MOPP (nitrogen mustard, vincristine, procarbazine, and prednisone) therapy with and without radiotherapy. *Hum Genet* 1994;**93**:295–299.

Brunet S, Maria AS, Guillaud P, Dujardin D, Kubiak JZ, Maro B. Kinetochore fibers are not involved in the formation of the first meiotic spindle in mouse oocytes, but control the exit from the first meiotic M phase. *J Cell Biol* 1999; **146**:1–12.

Chen HL, Tang CJ, Chen CY, Tang TK. Overexpression of an Aurora-C kinase-deficient mutant disrupts the Aurora-B/INCENP complex and induces polyploidy. *J Biomed Sci* 2005;**12**:297–310.

Cimini D, Wan X, Hirel CB, Salmon ED. Aurora kinase promotes turnover of kinetochore microtubules to reduce chromosome segregation errors. *Curr Biol* 2006;**16**:1711–1718.

DeLuca KF, Lens SM, DeLuca JG. Temporal changes in Hec1 phosphorylation control kinetochore-microtubule attachment stability during mitosis. *J Cell Sci* 2011;**124**:622–634.

Dieterich K, Soto Rifo R, Faure AK, Hennebicq S, Ben Amar B, Zahi M, Perrin J, Martinez D, Sele B, Jouk PS *et al.* Homozygous mutation of

AURKC yields large-headed polyploid spermatozoa and causes male infertility. *Nat Genet* 2007;**39**:661–665.

Dieterich K, Zouari R, Harbuz R, Vialard F, Martinez D, Bellayou H, Prisant N, Zoghmar A, Guichaoua MR, Koscinski I *et al*. The Aurora Kinase C c.144delC mutation causes meiosis I arrest in men and is frequent in the North African population. *Hum Mol Genet* 2009;**18**:1301–1309.

Edson MA, Nagaraja AK, Matzuk MM. The mammalian ovary from genesis to revelation. *Endocr Rev* 2009;**30**:624–712.

Ems-McClung SC, Hertzer KM, Zhang X, Miller MW, Walczak CE. The interplay of the N- and C-terminal domains of MCAK control microtubule depolymerization activity and spindle assembly. *Mol Biol Cell* 2007;**18**:282–294.

Fisher RA. *Statistical Methods for Research Workers*. Edinburgh: Oliver and Boyd, 1925.

Glover DM, Leibowitz MH, McLean DA, Parry H. Mutations in aurora prevent centrosome separation leading to the formation of monopolar spindles. *Cell* 1995;**81**:95–105.

Grondahl ML, Yding Andersen C, Bogstad J, Nielsen FC, Meinertz H, Borup R. Gene expression profiles of single human mature oocytes in relation to age. *Hum Reprod* 2010;**25**:957–968.

Gui L, Homer H. Spindle assembly checkpoint signalling is uncoupled from chromosomal position in mouse oocytes. *Development* 2012;**139**:1941–1946.

Hassold T, Hunt P. To err (meiotically) is human: the genesis of human aneuploidy. *Nat Rev Genet* 2001;**2**:280–291.

Hassold T, Hall H, Hunt P. The origin of human aneuploidy: where we have been, where we are going. *Hum Mol Genet* 2007;**16**(Spec No. 2):R203–R208.

Hu HM, Chuang CK, Lee MJ, Tseng TC, Tang TK. Genomic organization, expression, and chromosome localization of a third aurora-related kinase gene, Aie1. *DNA Cell Biol* 2000;**19**:679–688.

Igarashi H, Knott JG, Schultz RM, Williams CJ. Alterations of PLCbeta1 in mouse eggs change calcium oscillatory behavior following fertilization. *Dev Biol* 2007;**312**:321–330.

Illingworth C, Pirmadjid N, Serhal P, Howe K, Fitzharris G. MCAK regulates chromosome alignment but is not necessary for preventing aneuploidy in mouse oocyte meiosis I. *Development* 2010;**137**:2133–2138.

Imlay JA. Pathways of oxidative damage. *Ann Rev Microbiol* 2003;**57**:395–418.

Kimmins S, Crosio C, Kotaja N, Hirayama J, Monaco L, Hoog C, van Duin M, Gossen JA, Sassone-Corsi P. Differential functions of the Aurora-B and Aurora-C kinases in mammalian spermatogenesis. *Mol Endocrinol* 2007; **21**:726–739.

Kimura M, Matsuda Y, Yoshioka T, Okano Y. Cell cycle-dependent expression and centrosome localization of a third human aurora/Ipl1-related protein kinase, AIK3. *J Biol Chem* 1999;**274**:7334–7340.

Kline-Smith SL, Khodjakov A, Hergert P, Walczak CE. Depletion of centromeric MCAK leads to chromosome congression and segregation defects due to improper kinetochore attachments. *Mol Biol Cell* 2004; **15**:1146–1159.

Lampson MA, Renduchitala K, Khodjakov A, Kapoor TM. Correcting improper chromosome-spindle attachments during cell division. *Nat Cell Biol* 2004;**6**:232–237.

Lane SI, Yun Y, Jones KT. Timing of anaphase-promoting complex activation in mouse oocytes is predicted by microtubule-kinetochore attachment but not by bivalent alignment or tension. *Development* 2012;**139**:1947–1955.

Livak KJ, Schmittgen TD. Analysis of relative gene expression data using real-time quantitative PCR and the 2(-Delta Delta C(T)) Method. *Methods* 2001;**25**:402–408.

Matzuk MM, Lamb DJ. Genetic dissection of mammalian fertility pathways. *Nat Cell Biol* 2002;**4**(Suppl.):s41–s49.

Pacchierotti F, Adler ID, Eichenlaub-Ritter U, Mailhes JB. Gender effects on the incidence of aneuploidy in mammalian germ cells. *Environ Res* 2007; **104**:46–69.

Salimian KJ, Ballister ER, Smoak EM, Wood S, Panchenko T, Lampson MA, Black BE. Feedback control in sensing chromosome biorientation by the Aurora B kinase. *Curr Biol* 2011;**21**:1158–1165.

Sasai K, Katayama H, Stenoien DL, Fujii S, Honda R, Kimura M, Okano Y, Tatsuka M, Suzuki F, Nigg EA *et al*. Aurora-C kinase is a novel chromosomal passenger protein that can complement Aurora-B kinase function in mitotic cells. *Cell Motil Cytoskeleton* 2004;**59**:249–263.

Schindler K, Davydenko O, Fram B, Lampson MA, Schultz RM. Maternally recruited Aurora C kinase is more stable than Aurora B to support mouse oocyte maturation and early development. *Proc Natl Acad Sci USA* 2012;**109**:E2215–E2222.

Sharif B, Na J, Lykke-Hartmann K, McLaughlin SH, Laue E, Glover DM, Zernicka-Goetz M. The chromosome passenger complex is required for fidelity of chromosome transmission and cytokinesis in meiosis of mouse oocytes. *J Cell Sci* 2010;**123**:4292–4300.

Shuda K, Schindler K, Ma J, Schultz RM, Donovan PJ. Aurora kinase B modulates chromosome alignment in mouse oocytes. *Mol Reprod Dev* 2009;**76**:1094–1105.

Snedecor GW, Cochran WG. *Statistical Methods*, 8th edn. Ames Iowa: Iowa State University Press, 1989.

Sun SC, Zhang DX, Lee SE, Xu YN, Kim NH. Ndc80 regulates meiotic spindle organization, chromosome alignment, and cell cycle progression in mouse oocytes. *Microsc Microanal* 2011;**17**:431–439.

Takahashi T, Futamura M, Yoshimi N, Sano J, Katada M, Takagi Y, Kimura M, Yoshioka T, Okano Y, Saji S. Centrosomal kinases, HsAIRK1 and HsAIRK3, are overexpressed in primary colorectal cancers. *Jpn J Cancer Res* 2000;**91**:1007–1014.

Tang CJ, Lin CY, Tang TK. Dynamic localization and functional implications of Aurora-C kinase during male mouse meiosis. *Dev Biol* 2006;**290**:398–410.

Tsafriri A, Chun SY, Zhang R, Hsueh AJ, Conti M. Oocyte maturation involves compartmentalization and opposing changes of cAMP levels in follicular somatic and germ cells: studies using selective phosphodiesterase inhibitors. *Dev Biol* 1996;**178**:393–402.

Tseng TC, Chen SH, Hsu YP, Tang TK. Protein kinase profile of sperm and eggs: cloning and characterization of two novel testis-specific protein kinases (AIE1, AIE2) related to yeast and fly chromosome segregation regulators. *DNA Cell Biol* 1998;**17**:823–833.

Vogt E, Sanhaji M, Klein W, Seidel T, Wordeman L, Eichenlaub-Ritter U. MCAK is present at centromeres, midspindle and chiasmata and involved in silencing of the spindle assembly checkpoint in mammalian oocytes. *Mol Hum Reprod* 2010;**16**:665–684.

Wordeman L, Wagenbach M, von Dassow G. MCAK facilitates chromosome movement by promoting kinetochore microtubule turnover. *J Cell Biol* 2007; **179**:869–879.

Yan X, Wu Y, Li Q, Cao L, Liu X, Saiyin H, Yu L. Cloning and characterization of a novel human Aurora C splicing variant. *Biochem Biophys Res Commun* 2005;**328**:353–361.

Yanai A, Arama E, Kilfin G, Motro B. ayk1, a novel mammalian gene related to Drosophila aurora centrosome separation kinase, is specifically expressed during meiosis. *Oncogene* 1997;**14**:2943–2950.

Yang KT, Li SK, Chang CC, Tang CJ, Lin YN, Lee SC, Tang TK. Aurora-C kinase deficiency causes cytokinesis failure in meiosis I and production of large polyploid oocytes in mice. *Mol Biol Cell* 2010;**21**:2371–2383.

Yang KT, Lin YN, Li SK, Tang TK. Studying the roles of Aurora-C kinase during meiosis in mouse oocytes. *Methods Mol Biol* 2013;**957**: 189–202.

Zhang X, Lan W, Ems-McClung SC, Stukenberg PT, Walczak CE. Aurora B phosphorylates multiple sites on mitotic centromere-associated kinesin to spatially and temporally regulate its function. *Mol Biol Cell* 2007; **18**:3264–3276.